A Three-Dimensional Organoid Culture Model to Assess the Influence of Chemicals on Morphogenetic Fusion

David G. Belair,* Cynthia J. Wolf,* Sierra D. Moorefield,[†] Carmen Wood,* Carrie Becker,[†] and Barbara D. Abbott*,[1]

*Toxicity Assessment Division, National Health and Environmental Effects Research Laboratory, Office of Research and Development, US EPA, Research Triangle Park, North Carolina 27711; and [†]Oak Ridge Institute for Science and Education, Oak Ridge, Tennessee 37830

[1]To whom correspondence should be addressed at B105-4, 109 TW Alexander Drive, RTP, NC 27711. Tel: 919 541-2753; E-mail: abbott.barbara@epa.gov.

ABSTRACT

Embryologic development involves cell differentiation and organization events that are unique to each tissue and organ and are susceptible to developmental toxicants. Animal models are the gold standard for identifying putative teratogens, but the limited throughput of developmental toxicological studies in animals coupled with the limited concordance between animal and human teratogenicity motivates a different approach. *In vitro* organoid models can mimic the three-dimensional (3D) morphogenesis of developing tissues and can thus be useful tools for studying developmental toxicology. Common themes during development like the involvement of epithelial-mesenchymal transition and tissue fusion present an opportunity to develop *in vitro* organoid models that capture key morphogenesis events that occur in the embryo. We previously described organoids composed of human stem and progenitor cells that recapitulated the cellular features of palate fusion, and here we further characterized the model by examining pharmacological inhibitors targeting known palatogenesis and epithelial morphogenesis pathways as well as 12 cleft palate teratogens identified from rodent models. Organoid survival was dependent on signaling through EGF, IGF, HGF, and FGF pathways, and organoid fusion was disrupted by inhibition of BMP signaling. We observed concordance between the effects of EGF, FGF, and BMP inhibitors on organoid fusion and epithelial cell migration *in vitro*, suggesting that organoid fusion is dependent on epithelial morphogenesis. Three of the 12 putative cleft palate teratogens studied here (theophylline, triamcinolone, and valproic acid) significantly disrupted *in vitro* organoid fusion, while tributyltin chloride and all-trans retinoic acid were cytotoxic to fusing organoids. The study herein demonstrates the utility of the *in vitro* fusion assay for identifying chemicals that disrupt human organoid morphogenesis in a scalable format amenable to toxicology screening.

Key words: alternatives to animal testing; in vitro and alternatives, cell culture; in vitro and alternatives, developmental/teratology; reproductive and developmental toxicology.

The developmental program of the mammalian embryo involves a complex interplay between differentiating and self-organizing cells and tissues. The underlying mechanisms of organogenesis are unique to each tissue type and organ, but many tissues and organs rely upon common cellular and tissue events like epithelial-mesenchymal transition and tissue fusion (Ray and Niswander, 2012). Formation of the iris, urethra, heart, neural tube, and palate involves fusion of epithelial tissues, and the failure of tissue fusion can result in birth defects including coloboma formation, hypospadias, cardiac septal defects, neural tube defects, and cleft palate, respectively (Ray and Niswander, 2012). Developmental toxicity studies are carried out predominantly using animal models that have elucidated some of the signaling pathways and regulation involved in

---

mammalian development, but the limited throughput of animal models motivates alternative methods for toxicology. Furthermore, rodent models often provide limited usefulness in identifying human teratogens. An illustrative example is provided by thalidomide, which was shown in the 1960s to elicit profound birth defects in humans including phocomelia, but which exhibits no teratogenicity in many strains of rodents (Vargesson, 2015). Robust *in vitro* assays representative of human development are needed to screen putative teratogens and to parse the mechanisms of chemical teratogenicity.

In vitro assays using stem and progenitor cells are useful for examining mechanistic hypotheses about developmental toxicology, though *in vitro* models in general present a trade-off between throughput and developmental relevance (Yin et al., 2016). *In vitro* models are needed to provide enhanced throughput risk assessment and ultimately to reduce, refine, or replace vertebrate animal testing. These alternative methods, under the re-authorized Toxic Substances Control Act, require scaling and tissue-level complexity to recapitulate human biology and model responses to chemical exposures (Knudsen et al., 2017). Human organotypic culture models can recapitulate the cellular architecture of developmental tissues and to study the effect of suspected teratogens in a human-based *in vitro* system that is scalable and reproducible. Organoids composed of human stem or terminally differentiated cells can recapitulate skin, cornea, kidney, liver, cardiac, central nervous system, and gastrointestinal tissue and have increasingly been used in the context of toxicology (Lancaster and Knoblich, 2014). Organoids are useful for mimicking the cell-cell crosstalk and self-assembly involved in organogenesis, and these features are necessary for recapitulating tissue fusion events during development.

Palatogenesis involves the elevation, adhesion, and fusion of apposing palatal shelves during development (Ray and Niswander, 2012). Cleft palate results from the incomplete elevation or fusion of the palatal shelves and is a common craniofacial birth defects in humans (Mastroiacovo et al., 2011). The etiology of cleft palate involves both genetic and environmental factors (Abbott, 2010), which indicates the need for an organotypic model of morphogenetic fusion for identifying human cleft palate teratogens in reasonable throughput for screening. We previously reported on a method to robustly generate organoids composed of human stem and progenitor cells that mimicked the osteogenic phenotype and cellular architecture of embryonic palate. Organoid fusion *in vitro* recapitulated the cellular and morphologic features of palate fusion, specifically the EGF-dependent removal of epithelial cells from the seams between organoids and the formation of a confluent mesenchymal tissue (Belair et al., 2017). We sought here to explore the molecular mechanisms of organoid fusion and examine the sensitivity of the *in vitro* fusion assay to chemical challenge with known rodent cleft palate teratogens, some of which are teratogenic in humans. Organoid fusion was dependent on key palate fusion pathways including bone morphogenetic protein (BMP), epidermal growth factor (EGF), fibroblast growth factor (FGF), hepatocyte growth factor (HGF), and insulin-like growth factor (IGF) signaling. Additionally, valproic acid, theophylline, and triamcinolone disrupted organoid fusion, while tributyltin chloride and all-trans retinoic acid (ATRA) exerted cytotoxic effects on fusing organoids. Our results indicate that the organoid fusion model is sensitive to chemical disruption and serves as a useful tool to identify chemicals that disrupt morphogenetic fusion in a reproducible *in vitro* platform amenable to screening.

MATERIALS AND METHODS

Cell culture. Primary human Wharton's jelly stromal cells, HWJSCs (ATCC), were expanded, refrozen, and sub-cultured in HWJSC growth medium (GM), which contained mesenchymal stem cell (MSC) Basal Medium (ATCC PCS-500-030) supplemented with Mesenchymal Stem Cell Growth Kit for Adipose and Umbilical-derived MSCs—Low Serum (ATCC PCS-500-040). HWJSCs were passaged using Trypsin (ATCC) and Trypsin Neutralizer (ATCC) and counted by the Trypan blue dye exclusion method with the Countess Automated Cell Counter (Invitrogen). HWJSCs were used between passages 4 and 9 in experiments. Primary human epidermal keratinocyte progenitor cells, HPEKp (CellnTec), were expanded, refrozen, and sub-cultured in medium, CnT-PR (CellnTec). HPEKp were passaged using Accutase (CellnTec), counted as described above, and used between passages 4 and 9 in experiments.

Generation and osteogenic differentiation of HWJSC spheroids. Methods to generate agarose molds and HWJSC spheroids are described previously (Belair et al., 2017). Silicone molds, containing 300 microwells per well of a 24-well plate, were donated by William L. Murphy's laboratory at the University of Wisconsin. Agarose microwell molds were generated with molten 2% Ultra-Pure Agarose (Invitrogen) in Dulbecco's phosphate-buffered saline, DPBS (ATCC), and after solidification were placed into 24-well plate wells with 1 ml GM (supplemented with 1% antibiotic-antimycotic from Gibco), centrifuged at 2100 $\times$ g for 10 min, and incubated under normal culture conditions (37°C, 5% CO_2, 95% relative humidity). HWJSCs were stained with 10 μM CellTracker Orange Dye (Thermo Fisher Scientific) in GM for 20 min, and excess dye was removed following centrifugation at 200 $\times$ g for 5 min. HWJSCs were suspended and added at 0.3 $\times$ 10^6 cells/well in GM with 1% antibiotic-antimycotic to generate spheroids with 1000 cells/spheroid. HWJSCs were incubated in agarose microwells at room temperature for 5 min, centrifuged at 200 $\times$ g for 5 min, and incubated overnight under normal culture conditions. The following day, medium from each well was replaced with 0.75 ml/well of osteo-induction medium (OM) containing StemPro Osteogenesis Differentiation Kit (Gibco A1007201) supplemented with 1% antibiotic-antimycotic. HWJSCs were cultured in OM under normal culture conditions for 6 additional days, with medium changes every 2 days as described previously (Belair et al., 2017).

Generation of co-cultured HWJSC/HPEKp spheroids. A summary of the establishment of the organoid fusion model is provided in Figure 2. HWJSC spheroids after 7 days were harvested, washed in DPBS, suspended at 600 spheroids/ml in OM, and cultured for 2 h in ultra-low attachment 6-well plates (Corning) under normal culture conditions on an orbital shaker (~60 rpm). HWJSC spheroids were washed with DPBS and transferred to conical tubes for epithelial cell seeding. HPEKp were passaged and stained with 5 μM CellTracker Green (Thermo Fisher) in CnT-PR for 20 min under normal culture conditions. Excess dye was removed after centrifugation at 200 $\times$ g for 4 min, and HPEKp were washed once in DPBS and subsequently suspended in CnT-PR-CC (CellnTec) supplemented with 1% antibiotic-antimycotic. HPEKp were added at HPEKp/HWJSC cell ratios between 0.75 and 1.25 at 150 μl of HPEKp cell suspension per 600 HWJSC spheroids, and HWJSC spheroids + HPEKp were transferred to an ultra-low attachment 96-well plate (Corning). HWJSC spheroids + HPEKp were incubated for 6 h on an orbital shaker (~120 rpm) under normal culture conditions and were subsequently

transferred to a 6-well ultra-low attachment plate with 1.2 ml of CnT-PR-CC with 1% antibiotic-antimycotic and incubated overnight on an orbital shaker (~60 rpm) under normal culture conditions. A small volume of suspended HWJSC/HPEKp spheroids was analyzed with confocal laser scanning microscopy (Nikon A1), and z-stacks were processed to maximum intensity projections using NIS Elements (Nikon) to ensure the epithelial coverage was greater than 50% prior to experimentation.

Immunostaining organoids for vimentin and keratin 17. The immunostaining procedure was carried out as described previously (Belair *et al.*, 2017). Briefly, 24 h after the HPEKp were added to HWJSC spheroids, the resulting organoids were transferred to microcentrifuge tubes and fixed with 4% paraformaldehyde and 1% Triton X-100 (Sigma) in DPBS (pH 7.4, CellnTec) for 4 h rotating at 4°C. Fixed organoids were dehydrated/rehydrated with methanol (Fisher) in DPBS, blocked overnight in 3 wt.% BSA (Sigma) in DPBS-T containing 0.1% Triton X-100, stained with a 1:50 dilution of AlexaFluor 488-tagged antibodies against vimentin or keratin 17 (Abcam) for 48 h rotating at 4°C, and counter-stained with Hoechst 33256 (Life Technologies). Organoids were washed in DPBS-T overnight and imaged on Nikon A1R laser scanning confocal microscope.

Assessing the influence of chemicals on morphogenetic fusion in vitro. All chemicals were dissolved as a stock solution in DMSO (Fisher Scientific) and stored at −20°C until use. Chemical inhibitors CH5183284 (Nakanishi *et al.*, 2014), erlotinib (Moyer *et al.*, 1997), PHA665752 (Christensen *et al.*, 2003), K02288 (Sanvitale *et al.*, 2013), vismodegib (Wong *et al.*, 2011), XAV939 (Wang *et al.*, 2014), BMS536924 (Huang *et al.*, 2009), RO4929097 (Luistro *et al.*, 2009), and SB431542 (Dudas *et al.*, 2004) were purchased from Selleck Chemicals and used at a single concentration chosen based on literature. The test chemicals tretinoin (ATRA), fluconazole, corticosterone, triamcinolone acetonide, dexamethasone, caffeine, and valproic acid were purchased from Cayman Chemical. Tributyltin chloride, triadimefon, theophylline, and nicotine tartrate were purchased from Fisher Scientific. 2,3,7,8-tetrachlorodibenzo-*p*-dioxin (TCDD) was purchased as a stock solution in DMSO from Cambridge Isotope Laboratories. Staurosporine (positive control) was purchased as a 1 mM stock solution from Millipore Sigma. Chemicals (or DMSO vehicle control) were diluted to 0.2% from stock into CnT-PR-CC supplemented with 1% antibiotic-antimycotic and added to ultra-low attachment round bottom 96-well plates. For experiments examining the dependence of TCDD exposure on EGF signaling, TCDD was diluted to 0.31 µM (0.2% DMSO by volume) with recombinant human EGF (BioLegend) at 4 or 8 ng/ml in CnT-PR-CC with 1% antibiotic-antimycotic. HWJSC/HPEKp co-cultured spheroids were harvested and washed after 24 h of orbital shaker culture and suspended at 260 spheroids/ml in CnT-PR-CC (with 1% anti-anti). HWJSC/HPEKp spheroids were added at equal volume to the amount of chemical or vehicle control in each round bottom well at approximately 20 spheroids per well. Plates loaded with spheroids were centrifuged at $200 \times g$ for 2 min and were immediately imaged using Nikon A1 laser scanning confocal microscope using a 10X Plan Apo objective and lasers for 488 and 561 nm wavelengths. Fusion was monitored each day by confocal microscopy, and medium was replenished with chemicals, inhibitors, or controls (at 0.1% final concentration in CnT-PR-CC supplemented with 1% antibiotic-antimycotic) on day 2 of fusion. Relative cell viability was evaluated using CellTiter Glo 3D following the manufacturer's protocol as follows on fusion day 4. Medium in each well was

replaced with 100 µl per well of CellTiter Glo 3D reagent (Promega) that was diluted 1:1 in DPBS, and spheroids were incubated for 30 min on an orbital shaker under normal culture conditions. Reagent from each well was then transferred to a white 96-well plate (Falcon) and read on a luminescence plate reader with 10 s integration time per well (Clariostar BMG Labtech). Luminescence intensity from six replicate wells per condition was normalized to the DMSO control. One-way ANOVA with Dunnett *post-hoc* test was performed at $\alpha = 0.05$ for statistical significance using Prism software (GraphPad).

Fusion was assessed using morphometric analysis of a representative confocal optical section, approximately 40 µm from the bottom of the fusing organoids in each well, using NIS Elements v4.3 (Nikon). A region of interest was drawn around each sample, outlier pixels were removed through image processing, and a threshold was applied to each image uniformly. The Green/Red Area was calculated by processing each image to find the area of overlap between green and red channels (giving the area of green cells juxtaposed to red spheroids) and normalize the area of green in each image to the total area of red fluorescence only (i.e., red fluorescence that did not co-localize with green fluorescence) in each image. The Green/Red Area was calculated for each sample over time and normalized to the day 0 time point, giving a normalized Green/Red Area that was representative of the relative contribution of the epithelial cell area to the total organoid area in a given cross-section of the fusing organoids. A detailed description of the calculation of the Green/Red Area metric can be found in the Supplementary Methods file. Statistical analysis was performed using one-way ANOVA and Fisher's least significant difference test at a significance level of $\alpha = 0.05$.

Scratch assay of HPEKp migration. Human fibronectin (Corning) was used to coat wells in a 96-well optical bottom plate (Thermo Fisher Scientific) at 25 µg/ml for 1 h. HPEKp cells were stained with 10 µM CellTracker Green Dye in CnT-PR for 20 min. Excess dye was removed following centrifugation at $200 \times g$ for 5 min. HPEKp were suspended and added to fibronectin-coated 96-well plate at 3.3×10^4 cells/well in CnT-PR with 1% antibiotic-antimycotic. HPEKp cells were incubated at room temperature for 30 min and then incubated overnight under normal culture conditions.

The following day after seeding, the HPEKp cell monolayer was scratched using a 200-µl pipet tip held perpendicular to the surface of the plate. Wells were washed with 100 µL epithelial cell basal medium, CnT-PR-BM.1, following scratching (CellnTec). Each well was then filled with 150 µl of CnT-PR-CC medium with 1% antibiotic-antimycotic containing vehicle control (0.1% DMSO) or specified concentrations of test chemicals to make a final concentration of 0.1% DMSO in each well. The plate was immediately imaged on a Ti-Eclipse widefield fluorescence microscope (Nikon) using Plan Apo 10× objective, Sola light engine, Andor Neo VSC-01315 camera, and emission filter (522.5 nm) for green fluorescence. Wells were imaged on day 0, 1, and 2.

HPEKp migration was assessed using NIS Elements v4.3. A region of interest was drawn around each scratch area for each image taken on day 0. The region of interest for each well was then copied to each well's respective day 1 and day 2 images. Outlier pixels were removed through image processing for each image, and a threshold was applied to quantify the area of the region of interest covered by HPEKp. The total area covered by HPEKp for each sample was calculated for each time point and normalized to the vehicle control from at least three

independent experiments. Statistical analysis was performed using a two-way ANOVA and Dunnett's *post-hoc* multiple comparisons test at a significance level of $\alpha = 0.05$.

Relative cell viability in HPEKp scratch assays was determined using the CellTiter Glo assay (Promega) following the manufacturer's protocol. Immediately after imaging the plate at the 48 h time point, the medium in each well was replaced with 100 μl/well of CellTiter Glo reagent diluted 1:1 with DPBS. The plate was then incubated under normal culture conditions for 2 min while on an orbital shaker followed by a 10 min stationary incubation at room temperature. The reagent from each well was then mixed by pipetting, transferred to a white 96-well plate, and read on a luminescence plate reader with 10 s integration time per well. Luminescence intensity from three replicate wells per condition was normalized to the DMSO control. One-way ANOVA with a Dunnett's *post-hoc* multiple comparisons test was performed at $\alpha = 0.05$ for statistical significance.

Data accessibility. All meta data corresponding to the main text and supplementary data for this manuscript are publicly available at https://catalog.data.gov/organization/epa-gov under the title 'Data for 3D Organoid Model Assessment of Influence of Chemicals on Morphogenetic Fusion' and the unique identifier, A-n8q3.

RESULTS

Establishment of Organoid Fusion Model

Organoids composed of human stem and progenitor cells resembled the cytoarchitecture and phenotype of embryonic palatal tissue (osteogenic mesenchymal tissue surrounded by an epithelial layer) (Belair *et al.*, 2017), and organoid fusion *in vitro* mimicked the key cellular features of palate fusion—the removal of epithelial cells from the seams between organoids and the formation of a confluent mesenchymal tissue. The mesenchymal compartment of palate-like organoids was composed of human Wharton's jelly stromal cells (HWJSC) that self-aggregated into spheroids in nonadherent culture and were differentiated to the osteogenic lineage (Belair *et al.*, 2017). Neonatal epidermal keratinocyte progenitor cells (HPEKp) were seeded on the outer surface of osteogenic HWJSC spheroids. Organoids consisting of HWJSC and HPEKp stained positively for vimentin in the interior and keratin 17 on the periphery (Figure 1) consistent with the phenotype of embryonic palatal mesenchyme (Ferguson, 1988) and medial edge epithelium (Richardson *et al.*, 2017), respectively. Cell tracking dyes enabled live visualization of mesenchymal (red) and epithelial (green) cells in the organoids over time. Culture of organoids in round-bottom ultra-low attachment plates promoted organoids adhesion and initiated fusion that was tracked with confocal microscopy over time. Organoid viability was assessed by measuring relative ATP content at the end of the assay (Figure 2). Organoid fusion was characterized by the disappearance of epithelial cells from the seams between adjacent organoids and the formation of a confluent mesenchymal tissue (Figure 3A). The progression of fusion was quantified over time using the Green/Red Area metric (see Supplementary Methods). The Green/Red Area metric calculates the area of green fluorescence relative to the area of red fluorescence in a representative optical section through the fusing organoids in a given sample over time, normalized to day 0. The Green/Red Area quantitatively estimates the progression of fusion by taking into account the relative abundance of epithelial cells occupying a given cross

sectional area of a sample of fusing organoids. The metric is analogous to a perimeter to area ratio in two dimensions, which is a measure of the compactness of a two-dimensional shape, wherein the maximum compactness (ie, lowest perimeter to area ratio) is described by a circle (Li *et al.*, 2013). For example, at the beginning of fusion, the epithelial cells were present between all adjacent organoids, and at the end of fusion, the epithelial cells were restricted to the outside of the fused tissue while the resulting mesenchymal compartment was roughly twice the diameter of the mesenchymal compartment of an individual organoid at the start of fusion (Figure 3A). In this example, the perimeter to area ratio at the end of fusion equals half of the sum of the perimeter to area ratios of the individual organoids at the start of fusion (see Supplementary Methods). This calculation agrees with the observed Green/Red Area in the vehicle control that decreased significantly over time (ANOVA *p*-value < .01), specifically at days 2 and 4 relative to day 0, and reached a value of the Green/Red Area on day 4 that was 50% of its value at day 0 (Figure 3D). The Green/Red Area metric thus estimates the compactness of a sample of fusing organoids taking into account the relative architecture of the epithelial and mesenchymal tissue compartments.

Influence of Pharmacological Inhibitors on Organoid Fusion

We characterized the *in vitro* organoid fusion model and the fusion quantification method through a broad screen of a single concentration of pharmacological inhibitors against known epithelial morphogenesis pathways and palate fusion pathways: EGF, FGF, IGF, HGF, BMP, Wnt, sonic hedgehog (SHH), Notch, and transforming growth factor β (TGFβ). Two of the tested pharmacological inhibitors, K02288 (BMP inhibitor) (Figure 3B) and BMS536924 (IGF inhibitor) (Figure 3C), interfered with the morphogenesis of the fusing HWJSC/HPEKp organoids over time as indicated by the presence of HPEKp in the seams between fusing organoids at days 0, 1, 2, and 4. K02288 (Figure 3E) and BMS536924 (Figure 3F) treatment significantly increased the Green/Red Area relative to the DMSO control at day 4 and at days 1 and 2, respectively, which suggests that both treatments interfered with organoid fusion relative to the untreated control. Treated samples were compared with the DMSO control using the area under the curve (AUC) of the Green/Red Area after the first dose of chemical (days 0–2) and over the entire fusion process encompassing two doses (days 0–4). Treatment with either BMS536924 (IGF inhibitor) or erlotinib (EGF inhibitor) interfered with fusion during days 0–2 (Figure 4A), and BMS536924, erlotinib, K02288 (BMP inhibitor), PHA665752 (HGF inhibitor), and CH5183284 (FGF inhibitor) interfered with fusion during days 0–4 (Figure 4B), as indicated by the significantly higher normalized fusion AUC values versus the DMSO control over each respective time frame. However, at the doses studied, BMS536924, erlotinib, PHA665752, and CH5183284 reduced organoid viability significantly relative to the DMSO control at day 4 (Figure 4C), which suggests that BMP inhibition with K02288 specifically interfered with fusion, while IGF, EGF, HGF, or FGF inhibition interfered with organoid survival. Neither vismodegib (SHH inhibitor) nor XAV-939 (Wnt inhibitor) affected *in vitro* fusion, though RO4929097 (Notch inhibitor) reduced the normalized fusion AUC during days 0–2 (Figure 4A) and days 0–4 (Figure 4B) relative to the DMSO control, which suggests Notch inhibition accelerated fusion relative to the DMSO control. These results confirm that BMP signaling is critical to organoid morphogenesis and further highlight that the relative Green/Red Area and the normalized fusion AUC metrics are
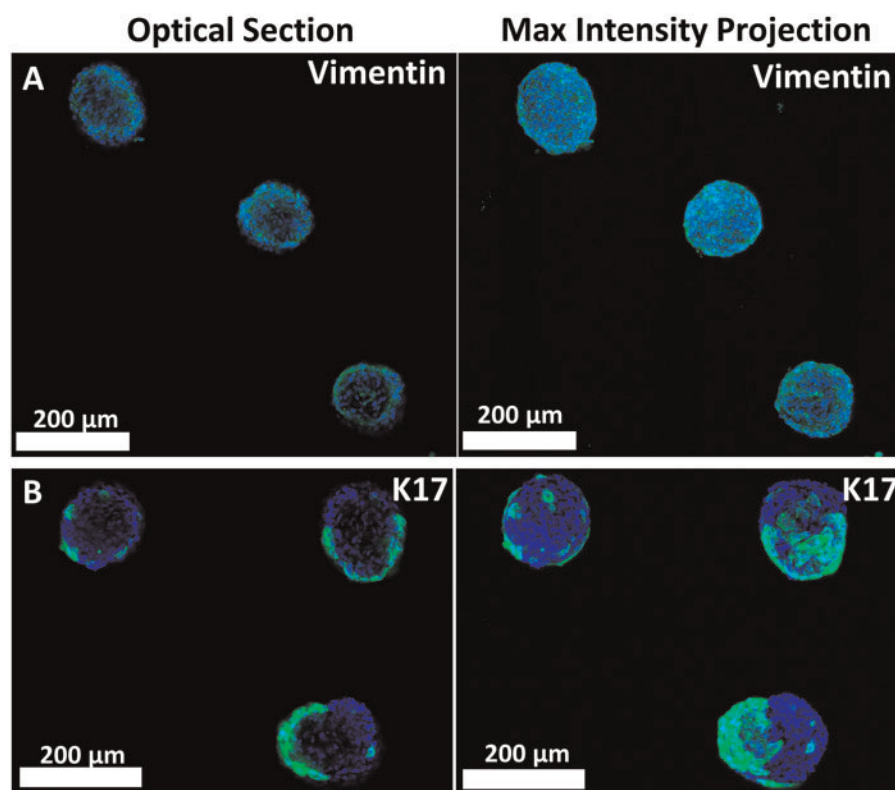
Figure 1. Immunostaining for vimentin and keratin 17 in organoids. Organoids were fixed and stained with AlexaFluor 488 tagged antibodies against vimentin (A) and keratin 17 (B), counter-stained with Hoechst, and imaged using confocal microscopy. A representative optical section and maximum intensity projection are presented.
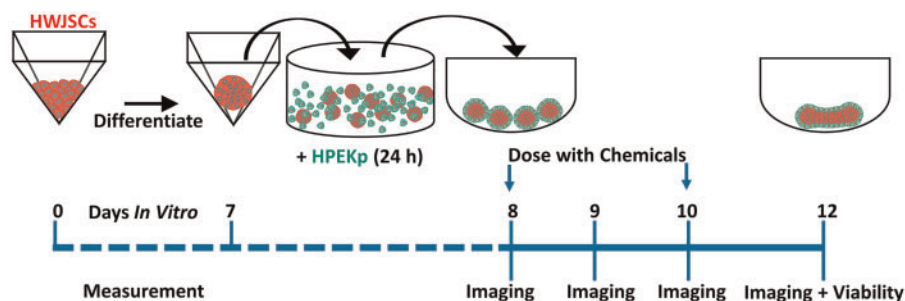

Figure 2. Establishment of the organoid fusion assay. Schematic of the generation of HWJSC spheroids, coating of HWJSC spheroids with HPEKp, and establishment of the fusion assay with HWJSC/HPEKp organoids, with the timeline indicating the culture time in days *in vitro* and the relevant measurements taken at each day. Organoid fusion was started on day 8 after the initial manufacturing of HWJSC spheroids, which corresponds to fusion day 0, and chemical dosing was performed on day 8 and 10, or day 0 and 2 of fusion.

sufficiently sensitive to identify chemical treatments that interfere with fusion.

Screening Rodent Cleft Palate Teratogens in the Organoid Fusion Model

The organoid fusion model was further characterized with a concentration-response analysis of 12 chemicals known to elicit cleft palate in rodent models. Our test chemicals included valproic acid, which is known to induce cleft palate teratogenicity in rodents and humans (Jentink *et al.*, 2010), as well as chemicals known to elicit cleft palate in rodents and whose putative molecular targets include CYP450 (fluconazole, triadimefon), nicotinic acetylcholine receptor (nicotine), adenosine receptor and phosphodiesterase (caffeine, theophylline), glucocorticoid receptor (dexamethasone, corticosterone, triamcinolone), retinoid

(RAR and RXR) receptors (ATRA and tributyltin, respectively), and aryl hydrocarbon receptor (TCDD). A summary of the influence of all 12 chemicals on organoid fusion is provided in Table 1. In the time window after initial dosing (days 0–2), valproic acid dose-dependently interfered with the fusion of palatal organoids and significantly increased the fusion AUC relative to the DMSO control at 50 and 0.5 µM (Figure 5B), while theophylline interfered with organoid fusion at a single concentration (1 µM) with no dose-dependent effect (Figure 5C). The normalized fusion AUC for valproic acid (Supplementary Figure 1A) and theophylline (Supplementary Figure 1B) was indistinguishable from control at days 0–4. Neither valproic acid (Figure 5H) nor theophylline (Figure 5I) affected organoid viability. Tributyltin chloride dose-dependently interfered with fusion after a single dose (days 0–2) (Figure 5A) and after two
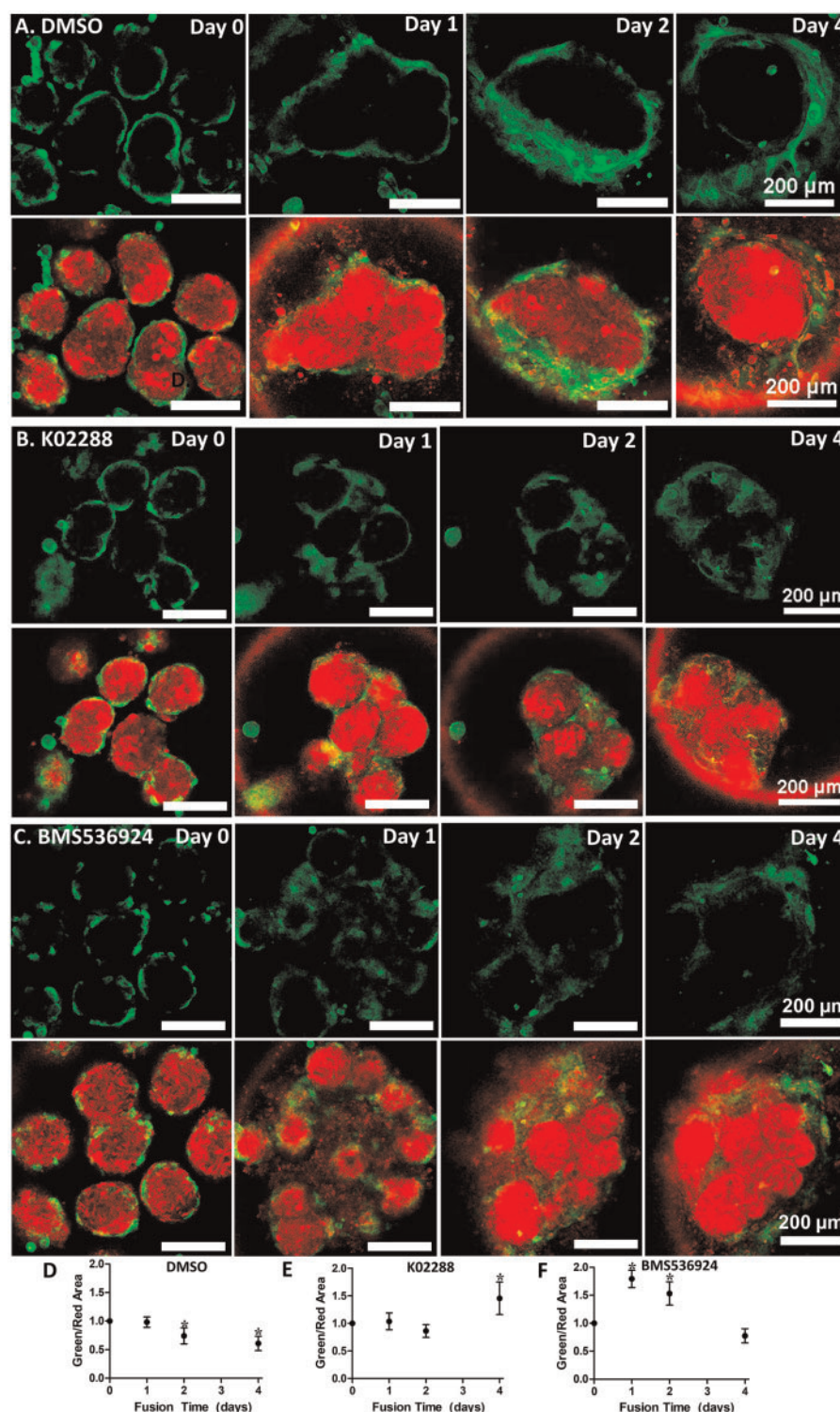
Figure 3. Characterization of the Green/Red Area metric for assessing fusion. A–C, Representative confocal optical sections of a representative sample treated with DMSO (A), 10 μM K02288 (B), or 1 μM BMS536924 (C) at days 0, 1, 2, and 4 of fusion showing the HPEKp channel alone (top row in A-C) or merged with the HWJSC channel (bottom row in A-C). D, Mean ± SEM of Green/Red Area over time throughout fusion of 9 samples aggregated from 3 independent experiments of DMSO-treated control, normalized to day 0. Asterisks denote statistical significance relative to day 0 using one-way ANOVA and Dunnett's *post-hoc* test ($\alpha = 0.05$). E and F, Mean ± SEM of Green/Red Area over time throughout fusion of 9 samples aggregated from 3 independent experiments from K02288 (E) or BMS536924 (F) treatment groups, normalized to day 0. Asterisks denote statistical significance using two-way ANOVA and Bonferroni *post-hoc* ($\alpha = 0.05$) test relative to DMSO control at each time point. For interpretation of the reference to color in this figure legend, the reader is referred to the web version of this article.

doses (days 0–4) (Figure 5D). Specifically, tributyltin chloride significantly affected the normalized fusion AUC at 5 and 50 μM after a single dose (0–2 days) and at 0.5 and 5 μM after two doses

(0–4 days) with no significant effect on fusion at 0.05 μM. Thus, the 0.5 μM concentration of tributyltin chloride only affected fusion after two doses of chemical (days 0–4) (Figure 5D). ATRA
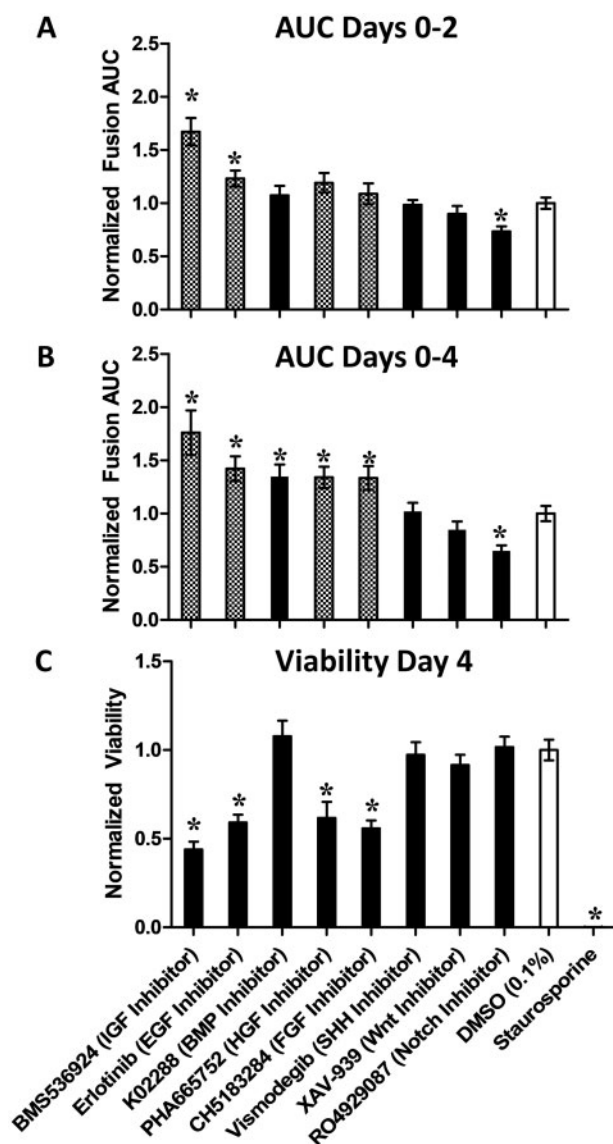
Figure 4. Influence of pharmacological inhibitors on organoid fusion. Organoids were treated with CH5183284 (10 μM), erlotinib (3 μM), PHA665752 (5 μM), K02288 (10 μM), vismodegib (10 μM), XAV-939 (5 μM), BMS-536924 (1 μM), RO4929097 (10 μM), staurosporine (1 μM), or DMSO (0.1%). A and B, Mean ± SEM, representing 9 samples aggregated across 3 independent experiments, of the fusion AUC for each treatment group normalized to the DMSO control for the day 0–2 time window (A) or for the day 0–4 time window (B). Asterisks denote statistical significance via one-way ANOVA and Fisher's least significant difference *post-hoc* test comparing each treatment group to the DMSO control at α = 0.05. C, Mean ± SEM, representing 18 samples aggregated across 3 independent experiments, of viability normalized to the DMSO control, calculated using CellTiter Glo 3D on day 4 of fusion. Staurosporine treatment (1 μM) served as a positive control for the viability assessment. For both the AUC and viability calculations, DMSO (0.1%) served as the negative control. Asterisks denote statistical significance via one-way ANOVA and Dunnett's *post-hoc* test comparing each treatment group to the DMSO control at α = 0.05.

and triamcinolone dose-dependently interfered with organoid fusion after two doses of chemical (days 0–4), although neither chemical significantly interfered with fusion after a single dose (days 0–2) (Supplementary Figs. 1C and D). ATRA significantly increased the normalized fusion AUC at 10 μM (days 0–4) (Figure 5E) whereas triamcinolone significantly reduced the normalized fusion AUC at 100 μM (days 0–4) relative to the DMSO

control (Figure 5F) during days 0–4 of fusion. Tributyltin chloride (Figure 5G) and ATRA (Figure 5J) both significantly affected viability in a dose-dependent fashion and reduced viability at the same concentrations at which an effect on fusion was observed, which suggests that cytotoxicity was associated with their influences on fusion. TCDD (Supplementary Figure 2), fluconazole, corticosterone, dexamethasone, caffeine, nicotine, and triadimefon (Supplementary Figure 3) did not influence organoid fusion or viability. These results together suggest that 5 out of the 12 chemicals tested here disrupted the progression of *in vitro* fusion (Table 1), and these data highlight the need for future studies examining putative cleft palate teratogens using the organoid fusion model.

Organoid fusion and viability were unaffected by TCDD exposure despite evidence that TCDD interferes with both mouse and human palatal explant fusion *in vitro*. TCDD did not affect the normalized fusion AUC at days 0–2 or 0–4 or organoid viability (Supplementary Figs. 2A–C). However, TCDD has been shown to interfere with the fusion of explanted mouse palatal shelves in an EGF-dependent manner, as TCDD only in the presence of 2 ng/ml recombinant EGF inhibited fusion of mouse palatal explants from EGF knockout mice *in vitro* (Abbott et al., 2005). We hypothesized that the supplementation of organoid fusion cultures with recombinant EGF would modify the responsiveness of TCDD in the organoid fusion model. Previously we showed that recombinant human EGF interfered with organoid fusion at 10 ng/ml, though 2 ng/ml EGF did not influence fusion (Belair et al., 2017). The highest non-cytotoxic dose of TCDD tested here (0.155 μM) by itself or supplemented with EGF at 2 or 4 ng/ml did not affect organoid fusion after a single dose (days 0–2), though the positive control (BMS536924, IGF inhibitor) interfered with fusion and significantly increased the normalized fusion AUC during the same time frame (Figure 6). These data demonstrate that the organoid fusion model here is insensitive to TCDD exposure. Future studies are needed to explore the sensitivity of the organoid fusion model to other putative cleft palate teratogens and interrogate the influence of variables like the timing of the dosing regimen and co-treatments that may modify the effect of chemicals *in vitro*.

Influence of Pharmacological Inhibitors and Putative Teratogens on Epithelial Migration

Given the dependence of the fusion model on epithelial morphogenesis pathways, we interrogated the influence of pharmacological inhibitors and test chemicals on HPEKp migration (Figs. 7A and B). RNA sequencing and immunostaining revealed that fibronectin was robustly expressed in HWJSC spheroids (Belair et al., 2017), thus we examined HPEKp migration using a scratch assay on fibronectin-coated plates to mimic the migration of epithelial cells between adjacent HWJSC spheroids during organoid fusion. Erlotinib, K02288, and BMS536924 significantly reduced epithelial cell migration at 24 h (Figure 7C) and 48 h (Figure 7D) after scratching in agreement with their inhibitory effects at the same respective concentrations tested on organoid fusion. However, erlotinib (Supplementary Figure 4A), CH5183284 (Supplementary Figure 4B), and RO4929097 significantly reduced HPEKp viability at the concentration tested, while neither K02288 nor BMS536924 affected HPEKp viability (Supplementary Figure 5A). Given that 0.5 μM erlotinib inhibited migration at 24 and 48 h and was cytotoxic at 48 h, we interrogated HPEKp viability at 0.5 μM after 24 h and observed no effect (Supplementary Figure 4C). Together, these results suggest that EGF signaling is indispensable for HPEKp migration (within the first 24 h) and survival (between 24 and 48 h), while FGF

Table 1. Summary of Test Chemical Effects on Epithelial Migration, Organoid Fusion, and Cell and Organoid Viability

Chemical	Δ Migration at 24 h	Δ Migration at 48 h	Δ HPEKp Viability	Δ Organoid Fusion Days 0–2	Δ Organoid Fusion Days 0–4	Δ Organoid Viability
Tributyltin	↓[a]	↓[a]	↓[a,b]	↓[a]	↓[a]	↓[a]
ATRA	↓[a]	↓[a]	↓[a]		↓[a]	↓[a]
Dexamethasone	↑[c]					
Corticosterone						
Triamcinolone		↓[c]			↑[a]	
Valproic acid				↓[a]		
Theophylline				↓[c,d]		
Caffeine						
Nicotine						
Fluconazole						
Triadimefon						
TCDD						

Arrows denote statistically significant increase or decrease relative to the DMSO control. Shaded rows indicate chemicals whose effects in the HPEKp migration assay and organoid fusion assay agreed (Tributyltin and ATRA) or disagreed (Dexamethasone, Triamcinolone, and Valproic Acid).
[a]Concentration-response-dependent change via one-way ANOVA.
[b]Reduced migration at and below 0.05 μM tributyltin was not associated with a significant change in viability.
[c]No concentration-response, but significant change at one concentration.
[d]Only effective at an intermediate concentration that was not tested in the HPEKp migration assay, thus no conclusion could be made related to the concordance of this result with the HPEKp migration assay.

signaling is indispensable for HPEKp survival during the entire assay time frame of 48 h. HPEKp migration was mediated by BMP and IGF signaling. These data agree with the EGF and FGF dependence of organoid survival and BMP dependence of organoid fusion. Neither PHA665752 (HGF inhibitor), vismodegib (SHH inhibitor), nor XAV939 (Wnt inhibitor) affected HPEKp viability or migration at the single concentration tested. We did not observe any influence of a TGFβR inhibitor, SB431542, on HPEKp migration (Figs. 7C and D), which suggests that HPEKp migration was independent of TGFβ signaling, in agreement with the TGFβ independence of organoid fusion as we previously demonstrated (Belair et al., 2017). ATRA (Figs. 8A–C) and tributyltin chloride (Figs. 8D–F) both reduced HPEKp migration and viability at the same concentrations that they were toxic to and inhibited organoid fusion. Tributyltin chloride at 0.05 and 0.005 μM reduced HPEKp migration at 24 h (Figure 8D) and 48 h (Figure 8E), respectively, and 0.05 μM tributyltin was toxic at 48 h (Figure 8F) but not 24 h after dosing (Supplementary Figure 4C), suggesting its effects at and below 0.05 μM were independent of cytotoxicity within the first 24 h after dosing. Dexamethasone increased HPEKp migration at 24 h (Figure 7E), and triamcinolone reduced HPEKp migration at 48 h relative to the DMSO control (Figure 7F, Table 1). Fluconazole, caffeine, valproic acid, theophylline, TCDD, corticosterone, nicotine, and triadimefon did not influence HPEKp migration (Figs. 7E and F) or viability (Supplementary Figure 5B) at the highest concentrations that were also tested in the organoid fusion assay. These results suggest that dexamethasone accelerated HPEKp migration, while triamcinolone, tributyltin chloride, and ATRA inhibited HPEKp migration, though ATRA and tributyltin chloride were cytotoxic to the HPEKp.

DISCUSSION

A major challenge in developmental toxicology is the evaluation of chemical effects in a model in vitro system that mimics the biology of human embryogenesis. Organoids composed of human stem cells can self-assemble into cellular architectures that mimic organogenesis (Lancaster and Knoblich, 2014) and are thus a useful tool for studying human developmental toxicity. Palate fusion is a complex three-dimensional morphogenesis process that historically has been studied in vitro using palate organ culture or two-dimensional cultures, and to date, no research group has attempted to model palate fusion using human cells in a physiologically relevant three-dimensional context. Here we report on a novel approach to examine the influence of putative teratogens in an in vitro organoid fusion model engineered using human stem and progenitor cells. We identified signaling pathways involved with in vitro fusion using pharmacological inhibitors targeting epithelial morphogenesis and palate fusion pathways, including EGF, FGF, HGF, IGF, BMP, SHH, Wnt, and Notch pathways. EGF and IGF inhibitors interfered with both early (days 0–2) and late (days 0–4) stages of fusion, but the reduced viability at day 4 suggests that EGF and IGF signaling were also indispensable for organoid survival. These data agree with the inhibitory and cytotoxic effect of both EGF and FGF inhibition on epithelial cell migration. The IGF inhibitor affected both organoid fusion (Figs. 3 and 4) and HPEKp migration (Figure 7), but significantly reduced viability only in the organoids without any change in viability of HPEKp monolayer cultures. These data suggest that IGF signaling is critical for HPEKp morphogenesis and that the cytotoxic effect of IGF inhibition on the organoids was likely through an effect on the HWJSCs. HWJSC spheroids were differentiated down the osteogenic lineage prior to addition of HPEKp and initiation of fusion, and the hypothesis that IGF inhibition reduced HWJSC viability in the fusion model is supported by studies demonstrating that IGF signaling promotes osteoblast proliferation (Guntur and Rosen, 2013; Zhang et al., 2012). The HGF and FGF inhibitors tested here were also cytotoxic to organoids and epithelial cells. The only pharmacological inhibitor in this study that significantly interfered with fusion and epithelial cell migration and did not affect cell viability was K02288 (Figs. 3 and 4), which inhibits ALK2 and ALK3 signaling (Sanvitale et al., 2013). Our results highlight the importance of BMP signaling specifically for epithelial morphogenesis during organoid fusion. BMP
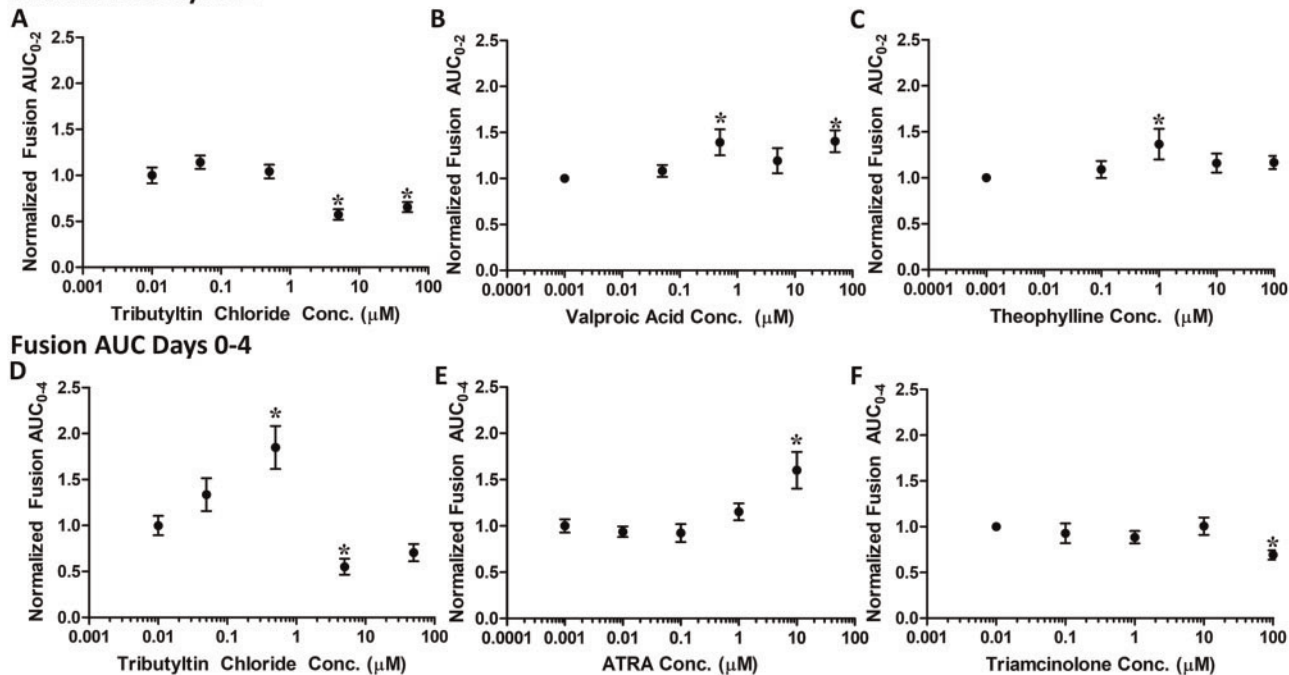
Figure 5. Influence of test chemicals on organoid fusion and viability. A–C, Mean ± SEM, representing 9 independent samples aggregated across 3 experiments, of the normalized fusion AUC for the day 0–2 time window upon treatment with a dose-response of tributyltin chloride (A), valproic acid (B), or theophylline (C). D–F: Mean ± SEM, representing 9 independent samples aggregated across 3 experiments, of the normalized fusion AUC for the day 0–4 time window upon treatment with a dose-response of tributyltin chloride (D), ATRA (E), or triamcinolone (F). Asterisks in A–F denote statistical significance via one-way ANOVA and Fisher's least significant difference *post-hoc* test comparing each dosage to the DMSO control (shown as the lowest concentration on each graph) at α = 0.05. G–K: Mean ± SEM, representing 18 independent samples aggregated across 3 experiments, of the viability (normalized to the DMSO control) upon treatment with tributyltin chloride (G), valproic acid (H), theophylline (I), ATRA (J), or triamcinolone (K). Asterisks in G–K denote statistical significance via one-way ANOVA and Dunnett's *post-hoc* test comparing each dosage to the DMSO control (shown as the lowest concentration on each graph) at α = 0.05. The positive control staurosporine (1 μM) significantly reduced organoid viability in each experiment.

signaling is known to be involved in rodent palate fusion (Gritli-Linde, 2007), and genetic polymorphisms involving the BMP pathway or downstream BMP signaling molecules have been associated with cleft palate in humans (Graf *et al.*, 2016; Parada and Chai, 2012). Here we present a method to examine organoid fusion in reasonable throughput for screening putative teratogens and discerning cytotoxic effects from disruption of human morphogenetic fusion.
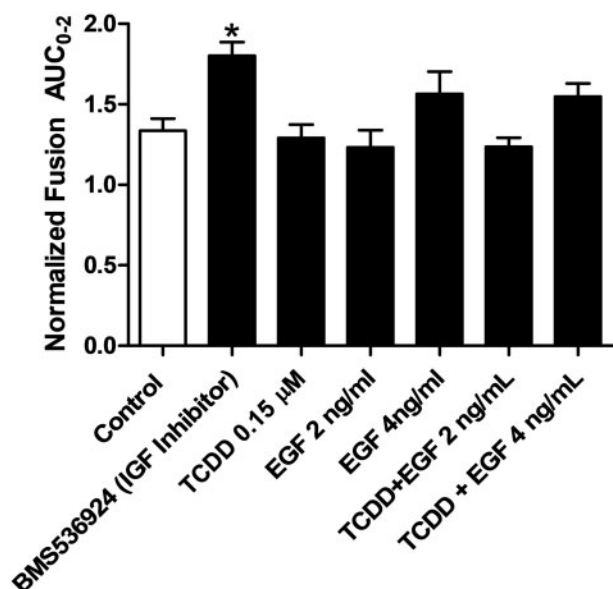
Figure 6. Influence of TCDD with or without supplemented EGF on organoid fusion. Mean ± SEM, representing at least 4 independent samples, of the normalized fusion AUC for the day 0–2 time window. Asterisks denote statistical significance via one-way ANOVA and Dunnett's *post-hoc* test comparing each treatment group to the DMSO control at $\alpha = 0.05$.

We examined the influence of 12 chemicals known to elicit cleft palate in rodent models and identified 5 that interfered with *in vitro* organoid fusion (Table 1). Out of the 12 chemicals screened, only 3 have been directly associated with cleft palate incidence in case studies in humans (valproic acid, retinoids, and fluconazole at high doses) (Schardein and Macina, 2006). Out of these three, we identified two (ATRA and valproic acid) that interfered with *in vitro* organoid fusion. Valproic acid dose-dependently disrupted *in vitro* fusion without any observed cytotoxicity, which agrees with the strong association between valproic acid exposure and fusion defects in humans, specifically cleft palate, spina bifida, atrial septal defects, and hypospadias (Jentink *et al.*, 2010). These observations suggest that valproic acid interferes with the cellular machinery underlying tissue fusion events during human embryonic development. Tributyltin chloride and ATRA were dose-dependently cytotoxic to organoids and epithelial cells in culture (Table 1) suggesting tributyltin and ATRA interfered with organoid fusion and HPEKp migration through cytotoxicity. However, tributyltin chloride at 0.05 µM inhibited HPEKp migration with no influence on viability 24 h (Figure 8D, Supplementary Figure 4C) while at 0.005 µM inhibited HPEKp migration with no influence on viability at 48 h (Figs. 8E and F) after scratching, which suggests the effects of tributyltin may be specific to interference of HPEKp migration. No controlled studies in humans have associated ATRA with cleft palate in humans, though the retinoid isotretinoin is directly associated with increased cleft palate incidence in humans (Willhite *et al.*, 1986). Similarly, no controlled studies to date have directly associated tributyltin with birth defects in humans, but tributyltin is a known developmental toxicant and cleft palate teratogen in rodent models (Ema *et al.*, 1995a,b; The Danish Environmental Protection Agency, 2013; U.S. Environmental Protection Agency, 1997). Both ATRA and tributyltin chloride were hits for RAR/RXR, PPAR, MMP1, THR, CXCL8, NR4A2 and NR1H4, and TP53 *via* their gene scores in ToxCast (Supplementary Table 1), which suggests an association

between these pathways and cytotoxicity in the organoid fusion model. The gene score is a metric assessing the effect of ToxCast chemicals on *in vitro* assays with specific pathway dependence that is independent from cell cytotoxicity and cell stress endpoints (Leung *et al.*, 2016). The gene scores associated with PPARα, RARβ, RARα, and RARγ were collectively the highest for both ATRA and tributyltin chloride, and thus it could be suggested that tributyltin chloride and ATRA induced cytotoxicity and thereby interfered with *in vitro* fusion through induction of the RAR/RXR or PPAR pathways. These outcomes motivate the study of other RAR/RXR agonists and antagonists in the organoid fusion model. Fluconazole did not influence organoid fusion or viability (Supplementary Figs. 3A–C), which agrees with the observed inactivity of fluconazole in ToxCast, wherein it exhibited a non-zero gene score for CYP2C19 and THRA (Supplementary Table 1), and neither of these pathways has been definitively associated with increased incidence of cleft palate in rodents or humans. Although numerous case studies have implicated fluconazole with human cleft palate (Schardein and Macina, 2006), the epidemiological literature does not agree on a statistical association between maternal fluconazole exposure and cleft palate incidence in humans (Mølgaard-Nielsen *et al.*, 2013). We identified that theophylline at a single intermediate dose interfered with *in vitro* fusion, though we observed no dose-response relationship *in vitro*, which agrees with the lack of a direct association between theophylline and cleft palate in humans. Triamcinolone elicited a dose-dependent decrease in the normalized fusion AUC in our *in vitro* fusion model, which suggests an increased rate of fusion relative to the DMSO control. None of the glucocorticoids studied here have been directly associated with cleft palate incidence in humans, although case studies have associated prednisolone, prednisone, and cortisol with cleft palate incidence in humans (Schardein, 2000). The observed interference of *in vitro* fusion with the highest dose of triamcinolone may be attributed to a weak positive dose-response relationship between triamcinolone and viability (ANOVA p-value = .052) (Figure 5K) that suggests triamcinolone increased cell survival or proliferation during spheroid fusion, and through its influence on cell proliferation, accelerated fusion. Our study demonstrates that the *in vitro* fusion model has the potential for identifying environmental and pharmacological chemicals that interfere with organoid survival and morphogenesis and motivates future studies to screen additional rodent cleft palate teratogens as well as suspected human teratogens.

Palate fusion involves coordinated activities of the palatal mesenchyme and medial edge epithelial (MEE) cells, and the etiology of genetic or chemical effects on palatogenesis involves effects on both the mesenchymal and epithelial cells that motivate the incorporation of epithelial-mesenchymal interactions into an *in vitro* model of morphogenetic fusion. During palatogenesis, midline epithelial seam degeneration is dependent on MEE cell migration, epithelial-mesenchymal transition, and apoptosis (Gritli-Linde, 2007; Jin and Ding, 2006), though the relative contribution of each towards palate fusion remains unclear (Abbott, 2010). We examined HPEKp viability and migration to further characterize whether chemical perturbation of organoid fusion may be mediated by effects on epithelial cell survival or migration. The organoid fusion and epithelial cell migration assays agree on the effect of EGF, FGF, and BMP inhibition. However, EGF inhibition was only cytotoxic after 48 h but not 24 h after scratching of the HPEKp monolayer (Supplementary Figure 4C), which suggests that EGF inhibition specifically inhibited migration in the first 24 h and was cytotoxic between 24
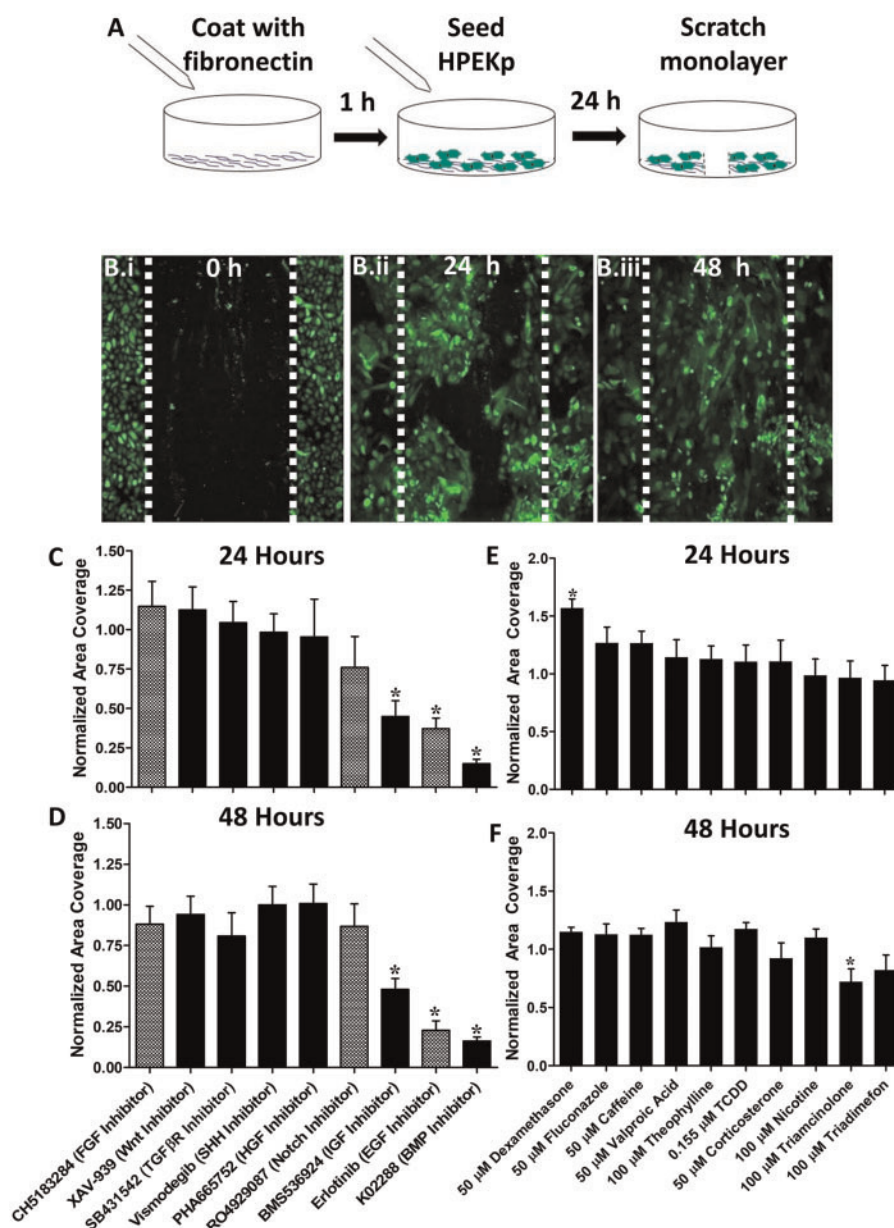
Figure 7. Establishment and characterization of the influence of pharmacological inhibitors on HPEKp migration. A, Schematic of HPEKp cell seeding on fibronectin coated plates followed by scratching. B, Epifluorescence micrographs of a representative DMSO-treated sample immediately after scratching (i), 24 h after scratching (ii), and 48 h after scratching (iii). C and D: Mean ± SEM, representing 9 samples aggregated across 3 independent experiments, of the area occupied by HPEKp in the scratch region normalized to the DMSO control 24 h after scratching (C) and 48 h after scratching (D) for a single concentration of pharmacological inhibitors. Cells were treated with CH5183284 (10 μM), erlotinib (0.5 μM), PHA665752 (5 μM), K02288 (10 μM), vismodegib (10 μM), XAV-939 (5 μM), BMS-536924 (1 μM), RO4929097 (20 μM), or DMSO (0.1%, omitted from the graph). E and F, Mean ± SEM, representing 9 samples aggregated across 3 independent experiments, of the area occupied by HPEKp in the scratch region normalized to the DMSO control 24 h after scratching (E) and 48 h after scratching (F) for test chemicals at a single concentration listed on the x-axis. Asterisks denote statistical significance comparing each treatment to the DMSO control via one-way ANOVA and Dunnett's *post-hoc* test at $\alpha = 0.05$.

and 48 h. The IGF inhibitor exhibited assay-dependent effects, as its inhibitory effect in the organoid fusion assay was associated with cytotoxicity whereas its inhibitory effect in the HPEKp migration assay was independent of cytotoxicity, suggesting IGF inhibition specifically interfered with HWJSC viability. The test chemicals consisting of putative teratogens also exhibited assay-dependent effects *in vitro*. Dexamethasone increased HPEKp migration at the tested concentration (50 μM) only at 24 h relative to the DMSO control, which suggests that dexamethasone increased the rate of HPEKp migration in the first 24 h after initiation of the scratch test, while dexamethasone had no

effect at this or lower concentrations in the organoid fusion model. Triamcinolone inhibited HPEKp migration at 48 h with exposure at 100 μM, while at this concentration triamcinolone accelerated organoid fusion, which suggests that the effect of triamcinolone on organoid fusion was likely through its influence on HWJSCs or paracrine signaling between HWJSCs and HPEKp. Finally, we did not observe any influence of valproic acid on HPEKp migration, which suggests that its inhibitory effect on *in vitro* organoid fusion may be due to a primary effect on the HWJSCs. The organoid fusion model identified differential effects of dexamethasone, valproic acid, triamcinolone, and
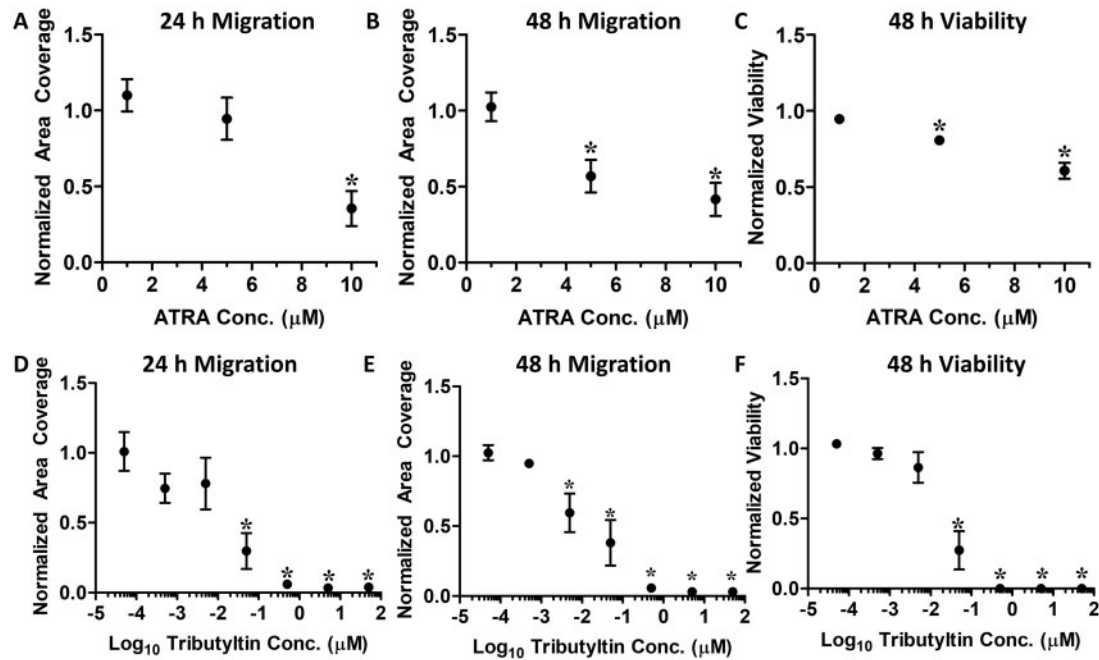
Figure 8. Influence of test chemicals on HPEKp migration. A and B, Mean ± SEM, representing 9 samples aggregated across 3 independent experiments, of the scratch area covered by HPEKp, relative to the DMSO control, upon treatment with a dose-response of ATRA, 24 h (A) or 48 h (B) after scratching. C, Mean ± SEM, representing 9 samples aggregated across 3 independent experiments, of the viability upon treatment with ATRA, relative to the DMSO control. D and E, Mean ± SEM, representing 9 samples aggregated across 3 independent experiments, of a dose-response of tributyltin chloride on the scratch area covered by HPEKp, normalized to the DMSO control 24 h (D) or 48 h (E) after scratching. F, Mean ± SEM, representing 9 samples aggregated across 3 independent experiments, of the viability upon treatment with tributyltin chloride relative to the DMSO control. Asterisks in A–F denote statistical significance comparing each concentration to the DMSO control via two-way ANOVA and Dunnett's *post-hoc* test at $\alpha = 0.05$.

IGF inhibition versus culture of epithelial cells alone, which supports incorporating epithelial-mesenchymal interactions into an *in vitro* model of palate fusion.

In vitro models can be used to study multiple aspects of morphogenetic tissue fusion and provide mechanistic insights about chemical exposures in a medium to high throughput fashion. The 12 chemicals screened here were identified as rodent cleft palate teratogens from the EPA database of animal toxicity studies, ToxRefDB (available online at https://doi.org/10.23645/epacomptox.6062545), and published rodent studies (Elmazar *et al.*, 1992; Ema et al., 1995a,b; Pratt *et al.*, 1984; Saad *et al.*, 1990; Shah and Kilistoff, 1976; Tiboni and Giampietro, 2005). *Ex vivo* rodent or human palatal organ cultures in suspension or on trans-well inserts have also been used to screen for cleft palate teratogenicity. Nine out of 12 of the rodent cleft palate teratogens here also inhibited fusion in rodent palatal organ culture *in vitro* (Abbott and Buckalew, 1992; Kang and Svoboda, 2003; Kosazuma *et al.*, 2004; Mino *et al.*, 1994). Kosazuma *et al.* screened fetal mouse palates in a suspension culture and identified ATRA, dexamethasone, caffeine, and theophylline as cleft palate teratogens *in vitro* (Kosazuma *et al.*, 2004), which agrees with the inhibitory effect of ATRA and theophylline that we observed in our organoid fusion model. Shimizu *et al.* identified that retinoic acid inhibited fusion of mouse palatal explants *in vitro* but did not elicit any effects on palatal shelf growth (Shimizu *et al.*, 2001), which agrees with the inhibitory effect of ATRA on organoid fusion here, although the effect on the organoids was likely mediated through cytotoxicity. Abbott and Buckalew identified that ATRA, dexamethasone, corticosterone, triamcinolone, and TCDD inhibited fusion of mouse palatal organs in suspension culture (Abbott and Buckalew, 1992). Human embryonic palatal organ culture has also been used to

study cleft palate teratogenicity *in vitro*, but these studies are limited by the availability of tissue. To our knowledge, only 2 out of the 12 rodent teratogens studied here, TCDD and ATRA, have been examined using human palatal organ culture, and both elicited cellular effects on palatal explants that would be expected to produce inhibition of fusion (Abbott *et al.*, 1998; Abbott and Birnbaum, 1991; Abbott and Pratt, 1987). We did not observe any *in vitro* inhibitory effects of TCDD, caffeine, dexamethasone, corticosterone, nicotine, fluconazole, or triadimefon on *in vitro* human organoid fusion (Table 1, Supplementary Figs. 2 and 3). The lack of response in the organoid fusion model to 7 of the 12 rodent teratogens studied here may also highlight potential differences between the dosing regimen used here versus previous *ex vivo* or *in vivo* palate fusion studies or species-dependent cellular responses that may underlie the lack of concordance between rodent studies and our human organoid fusion assay. Studies examining TCDD teratogenicity provide an illustrative example. TCDD promotes MEE cell proliferation during palatal shelf reorientation and alignment (Abbott and Birnbaum, 1991; Abbott *et al.*, 1989), which suggests that the teratogenicity of TCDD occurs prior to initiation of fusion. Future studies are needed to explore the influence of dosing prior to the initiation of fusion in the organoid fusion model on the effect of suspected teratogens. TCDD also interferes with palate fusion in an EGF-dependent fashion. In mice exposed to TCDD, the expression of EGFR was retained in the MEE while it was downregulated in untreated controls (Abbott and Birnbaum, 1989). In EGF knockout mice, TCDD interfered with fusion only in the presence of recombinant EGF (Abbott *et al.*, 2005). We did not observe any influence of TCDD (Supplementary Figure 2), either in the absence or presence of recombinant human EGF (Figure 6), in the organoid fusion

model. We confirmed that organoids expressed *AHR* (Supplementary Figure 2D), and across the TCDD dose-response, the expression of *AHR* was unaffected, in agreement with a prior study with mouse palatal explants (Abbott *et al.*, 1999). These data also agree with our previous study demonstrating with RNA sequencing that organoids expressed both *AHR* and *ARNT* (Belair *et al.*, 2017). However, organoids did not express measurable *CYP1A1* in control or TCDD-treated samples. We confirmed that the human *CYP1A1* primer could detect *CYP1A1* in primary human hepatocytes (data not shown), verifying that the lack of *CYP1A1* in organoids was biological. Although the organoids expressed AhR, CYP1A1, which is regulated by AhR, was not induced or expressed by the organoids, suggesting that AhR-mediated responses to TCDD were absent in organoids. It is possible that one or multiple components downstream of AhR/ARNT are missing in organoids, even though the organoids expressed measurable AhR transcripts. The insensitivity of the organoid fusion model to TCDD and other putative cleft palate teratogens may suggest that chemicals disrupting palatal shelf outgrowth or degeneration of the periderm prior to shelf adhesion do not influence organoid fusion. Prior to adhesion of the palatal shelves, the periderm layer covering the medial edge epithelium is removed *via* TGFβ signaling (Hu *et al.*, 2015), and the degeneration of the periderm layer is sensitive to disruption by chemicals including TCDD (Abbott and Birnbaum, 1991) and ATRA (Zhang *et al.*, 2017). Future iterations of the organoid fusion model are needed to assess the influence of chemicals on biological events that occur prior to palatal shelf fusion, including growth, elevation, and adhesion *in vitro*.

Rodent models are useful tools for identifying putative teratogens, however human and rodent development differ in several key aspects, and chemical teratogenicity in rodent models may not adequately predict teratogenicity in humans. For example, Abbott and colleagues demonstrated that the response of human palatal explants to TCDD exposure during *in vitro* fusion was three orders of magnitude less sensitive than the response of mouse palatal explants (Abbott *et al.*, 1999). This result suggests that TCDD may be a potent mouse cleft palate teratogen but may exhibit limited or no cleft palate teratogenicity in humans at a similar dose. This hypothesis is supported by evidence demonstrating that human AhR knock-in mice do not exhibit cleft palate upon TCDD exposure (Moriguchi *et al.*, 2003), suggesting species differences in AhR structure or activity may confer differential responsiveness of humans and mice to TCDD and other AhR agonists. The lack of definitive evidence of human teratogenicity for 9 out of the 12 rodent cleft palate teratogens here highlights the challenge in translating teratogenicity findings from rodent models with possible effects in humans and motivates future work to adapt human stem cell-based organoid systems to the study of developmental toxicity.

CONCLUSION

We used human stem and progenitor cells to engineer an organoid culture model that mimics the cellular architecture and phenotype of human embryonic palatal tissue and developed a quantitative real-time assay of organoid fusion. The *in vitro* organoid fusion assay was sensitive to disruption by 5 of the 12 rodent cleft palate teratogens studied here, which demonstrates sensitivity of the organoid fusion model for chemicals known to produce cleft palate in rodents. Future studies are needed to establish concordance or lack of concordance between the *in vitro* organoid fusion model, rodent palate organ culture models, and

epidemiological studies relating chemical exposures to cleft palate incidence in humans. Human stem cell-derived organoids can recapitulate complex cellular architecture and cell-cell crosstalk and are a useful tool for human developmental toxicity assessment.

SUPPLEMENTARY DATA

Supplementary data are available at *Toxicological Sciences* online.

Disclaimer

The information in this document has been funded wholly by the U.S. Environmental Protection Agency. It has been subjected to review by the National Health and Environmental Effects Research Laboratory and approved for publication. Approval does not signify that the contents reflect the views of the Agency, nor does mention of trade names or commercial products constitute endorsement or recommendation for use. The authors declare that no competing interests exist.

REFERENCES

Abbott, B. D. (2010). The etiology of cleft palate: A 50-year search for mechanistic and molecular understanding. *Birth Defects Res. Part B Dev. Reprod. Toxicol.* **89**, 266–274.

Abbott, B. D., and Birnbaum, L. S. (1989). TCDD alters medial epithelial cell differentiation during palatogenesis. *Toxicol. Appl. Pharmacol.* **99**, 276–286.

Abbott, B. D., and Birnbaum, L. S. (1991). TCDD exposure of human embryonic palatal shelves in organ culture alters the differentiation of medial epithelial cells. *Teratology* **43**, 119–132.

Abbott, B. D., and Buckalew, A. R. (1992). Embryonic palatal responses to teratogens in serum-free organ culture. *Teratology* **45**, 369–382.

Abbott, B. D., and Pratt, R. M. (1987). Human embryonic palatal epithelial differentiation is altered by retinoic acid and epidermal growth factor in organ culture. *J. Craniofac. Genet. Dev. Biol.* **7**, 241–265.

Abbott, B. D., Buckalew, A. R., and Leffler, K. E. (2005). Effects of epidermal growth factor (EGF), transforming growth factor-alpha (TGFalpha), and 2, 3, 7, 8-tetrachlorodibenzo-p-dioxin on fusion of embryonic palates in serum-free organ culture using wild-type, EGF knockout, and TGFalpha knockout mouse strains. *Birth Defects Res. A. Clin. Mol. Teratol.* **73**, 447–454.

Abbott, B. D., Diliberto, J. J., and Birnbaum, L. S. (1989). 2, 3, 7, 8-Tetrachlorodibenzo-p-dioxin alters embryonic palatal medial epithelial cell differentiation in vitro. *Toxicol. Appl. Pharmacol.* **100**, 119–131.

Abbott, B. D., Held, G. A., Wood, C. R., Buckalew, A. R., Brown, J. G., and Schmid, J. (1999). AhR, ARNT, and CYP1A1 mRNA quantitation in cultured human embryonic palates exposed to TCDD and comparison with mouse palate in vivo and in culture. *Toxicol. Sci.* **47**, 62–75.

Abbott, B. D., Probst, M. R., Perdew, G. H., and Buckalew, A. R. (1998). AH receptor, ARNT, glucocorticoid receptor, EGF receptor, EGF, TGFa, TGFb1, TGFb2, and TGFb3 expression in human embryonic palate, and effects of 2, 3, 7, 8-tetrachlorodibenzo-p-dioxin (TCDD). *Teratology* **58**, 30–43.

Belair, D. G., Wolf, C. J., Wood, C., Ren, H., Grindstaff, R., Padgett, W., Swank, A., MacMillan, D., Fisher, A., Winnik, W., *et al.* (2017). Engineering human cell spheroids to model embryonic tissue fusion in vitro. *PLoS One* **12**, e0184155–e0184131.

Christensen, J. G., Schreck, R., Burrows, J., Kuruganti, P., Chan, E., Le, P., Chen, J., Wang, X., Ruslim, L., Blake, R., *et al.* (2003). A selective small molecule inhibitor of c-Met kinase inhibits c-Met-dependent phenotypes in vitro and exhibits cytoreductive antitumor activity in vivo. *Cancer Res.* **63**(21), 7345–55.

Dudas, M., Nagy, A., Laping, N. J., Moustakas, A., and Kaartinen, V. (2004). Tgf-β3-induced palatal fusion is mediated by Alk-5/Smad pathway. *Dev. Biol.* **266**, 96–108.

Elmazar, M. M., Thiel, R., and Nau, H. (1992). Effect of supplementation with folinic acid, vitamin B6, and vitamin B12 on valproic acid-induced teratogenesis in mice. *Toxicol. Sci.* **18**, 389–394.

Ema, M., Kurosaka, R., Amano, H., and Ogawa, Y. (1995a). Comparative developmental toxicity of butyltin trichloride, dibutyltin dichloride and tributyltin chloride in rats. *J. Appl. Toxicol.* **15**, 297–302.

Ema, M., Kurosaka, R., Amano, H., and Ogawa, Y. (1995b). Further evaluation of the developmental toxicity of tributyltin chloride in rats. *Toxicology* **96**, 195–201.

Ferguson, M. W. (1988). Palate development. *Development* **103**(Suppl), 41–60.

Graf, D., Malik, Z., Hayano, S., and Mishina, Y. (2016). Common mechanisms in development and disease: BMP signaling in craniofacial development. *Cytokine Growth Factor Rev.* **27**, 129–139.

Gritli-Linde, A. (2007). Molecular control of secondary palate development. *Dev. Biol.* **301**, 309–326.

Guntur, A. R., and Rosen, C. J. (2013). IGF-1 regulation of key signaling pathways in bone. *Bonekey Rep.* **2**, 1–6.

Hu, L., Liu, J., Li, Z., Ozturk, F., Gurumurthy, C., Romano, R.-A., Sinha, S., and Nawshad, A. (2015). TGFbeta3 regulates periderm removal through DeltaNp63 in the developing palate. *J. Cell. Physiol.* **230**, 1212–1225.

Huang, F., Greer, A., Hurlburt, W., Han, X., Hafezi, R., Wittenberg, G. M., Reeves, K., Chen, J., Robinson, D., Li, A., *et al.* (2009). The mechanisms of differential sensitivity to an insulin-like growth factor-1 receptor inhibitor (BMS-536924) and rationale for combining with EGFR/HER2 inhibitors. *Cancer Res.* **69**, 161–170.

IPDTOC Working Group. (2011). Prevalence at birth of cleft lip with or without cleft palate: data from the International Perinatal Database of Typical Oral Clefts (IPDTOC). *Cleft Palate Craniofac J.* **48**(1):66–81.

Jentink, J., Loane, M. A., Dolk, H., Barisic, I., Garne, E., Morris, J. K., and de Jong-van den Berg, L. T. W. (2010). Valproic acid monotherapy in pregnancy and major congenital malformations. *N. Engl. J. Med.* **362**, 2185–2193.

Jin, J., and Ding, J. (2006). Analysis of cell migration, transdifferentiation and apoptosis during mouse secondary palate fusion. *Development* **133**, 3341–3347.

Kang, P., and Svoboda, K. K. H. (2003). Nicotine inhibits palatal fusion and modulates nicotinic receptors and the PI-3 kinase pathway in medial edge epithelia. *Orthod. Craniofac. Res.* **6**, 129–142.

Knudsen T. B, Klieforth B., Slikker W. Jr. (2017). Programming microphysiological systems for children's health protection. *Exp Biol Med (Maywood).* **242**(16), 1586–1592.

Kosazuma, T., Hashimoto, S., Ohno, H., Chou, M.-J., and Shiota, K. (2004). Organ culture of the fetal mouse palate for screening the developmental toxicity of chemicals: A validation study. *Congenit. Anom.* **44**, 60–71.

Lancaster, M. A., and Knoblich, J. A. (2014). Organogenesis in a dish: Modeling development and disease using organoid technologies. *Science* **345**, 1247125.

Leung, M. C., Phuong, J., Baker, N. C., Sipes, N. S., Klinefelter, G. R., Martin, M. T., McLaurin, K. W., Setzer, R.W., Darney, S. P., Judson, R. S., Knudsen, T. B. (2016). Systems Toxicology of Male Reproductive Development: Profiling 774 Chemicals for Molecular Targets and Adverse Outcomes. *Environ Health Perspect.* **124**(7), 1050–1061.

Li, W., Goodchild, M. F., and Church, R. (2013). An efficient measure of compactness for two-dimensional shapes and its application in regionalization problems. *Int. J. Geogr. Inf. Sci.* **27**, 1227–1250.

Luistro, L., He, W., Smith, M., Packman, K., Vilenchik, M., Carvajal, D., Roberts, J., Cai, J., Berkofsky-Fessler, W., Hilton, H., *et al.* (2009). Preclinical profile of a potent gamma-secretase inhibitor targeting notch signaling with in vivo efficacy and pharmacodynamic properties. *Cancer Res.* **69**(19), 7672–80.

Mino, Y., Mizusawa, H., and Shiota, K. (1994). Effects of anticonvulsant drugs on fetal mouse palates cultured in vitro. *Reprod. Toxicol.* **8**, 225–230.

Mølgaard-Nielsen, D., Pasternak, B., and Hviid, A. (2013). Use of oral fluconazole during pregnancy and the risk of birth defects. *N. Engl. J. Med.* **369**, 830–839.

Moriguchi, T., Motohashi, H., Hosoya, T., Nakajima, O., Takahashi, S., Ohsako, S., Aoki, Y., Nishimura, N., Tohyama, C., Fujii-Kuriyama, Y., *et al.* (2003). Distinct response to dioxin in an arylhydrocarbon receptor (AHR)-humanized mouse. *Proc. Natl. Acad. Sci. U.S.A.* **100**, 5652–5657.

Moyer, J. D., Barbacci, E. G., Iwata, K.K., Arnold, L., Boman, B., Cunningham, A., DiOrio, C., Doty, J., Morin, M. J., Moyer, M. P., *et al.* (1997). Induction of apoptosis and cell cycle arrest by CP-358,774, an inhibitor of epidermal growth factor receptor tyrosine kinase. *Cancer Res.* **57**(21), 4838–48.

Nakanishi, Y., Akiyama, N., Tsukaguchi, T., Fujii, T., Sakata, K., Sase, H., Isobe, T., Morikami, K., Shindoh, H., Mio, T., *et al.* (2014). The fibroblast growth factor receptor genetic status as a potential predictor of the sensitivity to CH5183284/debio 1347, a novel selective FGFR inhibitor. *Mol. Cancer Ther.* **13**, 2547–2558.

Parada, C., and Chai, Y. (2012). Roles of BMP Signaling pathway in lip and palate development. *Front. Oral Biol.* **16**, 60–70.

Pratt, R. M., Dencker, L., and Diewert, V. M. (1984). 2, 3, 7, 8-Tetrachlorodibenzo-p-dioxin- induced cleft palate in the mouse: Evidence for alterations in palatal shelf fusion. *Teratog. Carcinog. Mutagen.* **4**, 427–436.

Ray, H. J., and Niswander, L. (2012). Mechanisms of tissue fusion during development. *Development* **139**, 1701–1711.

Richardson, R., Mitchell, K., Hammond, N. L., Mollo, M. R., Kouwenhoven, E. N., Wyatt, N. D., Donaldson, I. J., Zeef, L., Burgis, T., Blance, R., *et al.* (2017). p63 exerts spatio-temporal control of palatal epithelial cell fate to prevent cleft palate. *PLoS Genet.* **13**(6), e1006828.

Saad, A. Y., Gartner, L. P., and Hiatt, J. L. (1990). Teratogenic effects of nicotine on palate formation in mice. *Biol. Struct. Morphog.* **3**, 31–35.

Sanvitale, C. E., Kerr, G., Chaikuad, A., Ramel, M.-C., Mohedas, A. H., Reichert, S., Wang, Y., Triffitt, J. T., Cuny, G. D., Yu, P. B., *et al.* (2013). A new class of small molecule inhibitor of BMP signaling. *PLoS One* **8**, e62721.

Schardein, J. L. (2000). *Chemically Induced Birth Defects*. Dekker, New York.

Schardein, J. L., and Macina, O. T. (2006) *Human Developmental Toxicants: Aspects of Toxicology and Chemistry*. New York: CRC Press.

Shah, R. M., and Kilistoff, A. (1976). Cleft palate induction in hamster fetuses by glucocorticoid hormones and their synthetic analogues. *J. Embryol. Exp. Morphol*. **36**, 101.

Shimizu, N., Aoyama, H., Hatakenaka, N., Kaneda, M., and Teramoto, S. (2001). An in vitro screening system for characterizing the cleft palate-inducing potential of chemicals and underlying mechanisms. *Reprod. Toxicol*. **15**, 665–672.

The Danish Environmental Protection Agency. (2013). Tributyltin compounds (TBT). Evaluation of health hazards and proposal of health based quality criteria for soil and drinking water.

Tiboni, G. M., and Giampietro, F. (2005). Murine teratology of fluconazole: Evaluation of developmental phase specificity and dose dependence. *Pediatr. Res*. **58**, 94.

U.S. Environmental Protection Agency. (1997). Toxicological review of tributyltin oxide. Available at: https://cfpub.epa.gov/ncea/iris2/chemicalLanding.cfm?substance_nmbr=349.

Vargesson, N. (2015). Thalidomide-induced teratogenesis: History and mechanisms. *Birth Defects Res. Part C Embryo Today Rev*. **105**, 140–156.

Wang, C., Zhu, H., Sun, Z., Xiang, Z., Ge, Y., Ni, C., Luo, Z., Qian, W., and Han, X. (2014). Inhibition of Wnt/-catenin signaling promotes epithelial differentiation of mesenchymal stem cells and repairs bleomycin-induced lung injury. *AJP Cell Physiol*. **307**, C234–C244.

Willhite, C. C., Hill, R. M., Irving, D. W. (1986). Isotretinoin-induced craniofacial malformations in humans and hamsters. *J Craniofac Genet Dev Biol* Suppl. **2**, 193–209.

Wong, H., Alicke, B., West, K. A., Pacheco, P., La, H., Januario, T., Yauch, R. L., de Sauvage, F. J., and Gould, S. E. (2011). Pharmacokinetic-pharmacodynamic analysis of vismodegib in preclinical models of mutational and ligand-dependent Hedgehog pathway activation. *Clin. Cancer Res*. **17**, 4682–4692.

Yin, X., Mead, B. E., Safaee, H., Langer, R., Karp, J. M., and Levy, O. (2016). Engineering stem cell organoids. *Cell Stem Cell* **18**, 25–38.

Zhang, W., Shen, X., Wan, C., Zhao, Q., Zhang, L., Zhou, Q., and Deng, L. (2012). Effects of insulin and insulin-like growth factor 1 on osteoblast proliferation and differentiation: differential signalling via Akt and ERK. *Cell Biochem. Funct*. **30**, 297–302.

Zhang, Y.-D., Dong, S.-Y., & Huang, H.-Z. (2017). Inhibition of periderm removal in all-trans retinoic acid-induced cleft palate in mice. *Experimental and Therapeutic Medicine*, **14**(4), 3393–3398.